[ECCE]-Coordinated (E = P, As) Ruthenium Complexes in Different Oxidation States: Ru(I) (E = P), Ru(II) (E = P, As) and Ru(III) (E = As)

Benjamin Rudin, Carolin A. M. Stein and Joachim Ballmann*

Anorganisch-Chemisches Institut, Universität Heidelberg, Im Neuenheimer Feld 276, D-69120 Heidelberg, Germany.

Supporting Information Placeholder

ABSTRACT: Targeting Ru(III) and Ru(I) η^2-alkyne complexes, 2,2'-(^{i}Pr$_2$E)$_2$-substituted diphenylacetylenes (1-E, E = P, As) were employed for the preparation of [ECCE]-coordinated Ru(II) complexes, which were examined with respect to 1e^- oxidation and reduction. Starting from [(η^6-cymene)RuCl$_2$]$_2$ and 1-E, ligand cyclization reactions (via attack of one ^{i}Pr$_2$E moiety at the alkyne) were observed and found to afford cyclic aryl ylidic mesoionic carbenes (2-E). Attempts to ring-open these complexes were unsuccessful for E = P, but found to proceed smoothly for E = As, which led to the isolation of *cis*-[AsCCAs]RuCl$_2$(MeCN) (3-As). To also gain access to the corresponding [PCCP]-coordinated derivative (3-P), the reactions between 1-E (E = P, As) and *cis*-(MeCN)$_2$(COD)RuCl$_2$ · 2 MeCN were examined, which led to the envisioned complexes 3-E for E = As and E = P. Compounds *cis*-[ECCE]RuCl$_2$(MeCN) (3-E) and their carbonyl derivatives *cis*-[ECCE]RuCl$_2$(CO) (5-E) were oxidized using PhICl$_2$, which led to an oxidative dichlorination of the alkyne in the case of 5-E. The latter dichlorination was found to occur *trans*-selective to afford complexes of the type [*trans*-E(Cl)C=C(Cl)E]RuCl$_2$(CO) (6-E), while unselective oxidation processes set in upon treatment of 3-E with PhICl$_2$. Although the envisioned Ru(III) complexes [ECCE]RuCl$_3$ (7-E) were detectable for E = P and E = As, only the *arsa*-derivative 7-As was obtained in a pure form, namely via oxidation of *cis*-[ECCE]RuCl$_2$(THT) (8), which is accessible for E = As only. Upon reduction of compounds 3-E, a hitherto unprecedented Ru(I) η^2-alkyne complex, [PCCP]RuCl (9), was obtained for E = P, while multiple attempts to also isolate the corresponding *arsa*-derivative met with failure. The former square planar Ru(I) complex (9) was characterized comprehensibly and examined in detail by means of DFT and CASSCF calculation. Upon treatment of 9 with TlPF$_6$, a diamagnetic μ-Tl-bridged compound (10) with a nearly linear Ru–Tl–Ru array was formed and isolated in high yields. Careful analysis of the bonding situation suggested that the Ru–Tl–Ru moiety in 10 is best interpreted in terms of a 3*c*-4e^- bond.

INTRODUCTION

Ruthenium-catalyzed transformation of internal and terminal alkynes, such as hydroelementation reactions are highly valued in organic synthesis and widely applied to selectively forge new element-carbon bonds.[1] Due to the high kinetic stability of ruthenium(II) and its propensity to undergo 2e^- redox reactions,[2] it is not too surprising that most ruthenium-catalyzed alkyne transformations either rely on redox-neutral steps in conjunction with an even-electron Ru catalyst or on the interplay between Ru(II) and Ru(0).[3] For both the latter oxidation states, numerous η^2-alkyne complexes have been isolated and comprehensively characterized,[4] which certainly added its share to our contemporary understanding of the aforementioned transformations. Along these lines, it is of fundamental interest to also expand our knowledge on Ru(I) and Ru(III) η^2-alkyne complexes and thus lay a foundation to either truly excluded or actually identify these species in catalysis.[5] In this context, Bennett and coworkers set out to prepare the first Ru(III) η^2-alkyne complex (B) via 1e^- oxidation of the corresponding Ru(II) derivative (A, see Figure 1).[6] Interestingly, an inspection of the Ru–C distances in A and B suggested that the alkyne in B is more strongly bound than the alkyne in A,[6] while an opposite trend has been uncovered for closely related Ru η^2-olefine complexes.[7]

Considering that no other pair of Ru(II)/Ru(III) η^2-alkyne complexes has been characterized crystallographically in both relevant oxidation states, we became interested in corroborating Bennett's results by using our (potentially tridentate) 2,2'-diphosphinotolane scaffold (1-P, see Figure 1)[8] for the synthesis of Ru(III) η^2-alkyne complexes.

Due to the presence of two phosphines in 1-P, we speculated that this approach may also allow for the synthesis of a hitherto unknown Ru(I) η^2-alkyne complex. In this context, it needs to be noted that all the yet known mononuclear Ru(I) complexes actually contain phosphines,[9, 10] but differ in their valence electron counts and in their geometries. While Peters and others succeeded in isolating trigonal bipyramidal 17-valence-e^- Ru(I) complexes,[9a, c, e] Grützmacher reported a unique 15-valence-e^- Ru(I) complex in a square planar coordination environment.[9d] The latter 15-valence-e^- Ru(I) complex (D) comprises two coordinated olefins and two mutually *cis*-positioned phosphines, while an η^6-arene interaction (between the metal and one of the arenes in tropPPh$_2$, see Figure 1) was found in the corresponding Ru(II) counterpart (C).[9d] Given that these stereochemical peculiarities interfere with an unambiguous comparison of C and D, our strategy to employ a rigid tridentate scaffold (such as 1-P) for the synthesis of mutually comparable Ru(I), Ru(II) and

Ru(III) η^2-alkyne complexes seemed reasonable, at least at a first glance.

Previous studies, however, revealed that1-P is prone to intramolecular cyclization via attack of one of the phosphines at the central alkyne, which may result in the formation of *P*-ylidic species instead of (or in addition to) the envisioned pincer-type complexes.[11] Given that similar cyclization reactions are commonly not encountered for the *arsa*-derivative 1-As (due to the lower thermodynamic stability of *As*-ylides),[12] we decided to also include 1-As in our studies and thus higher the chances to indeed access [ECCE]-coordinated Ru(I) and Ru(III) complexes (E = P, As).

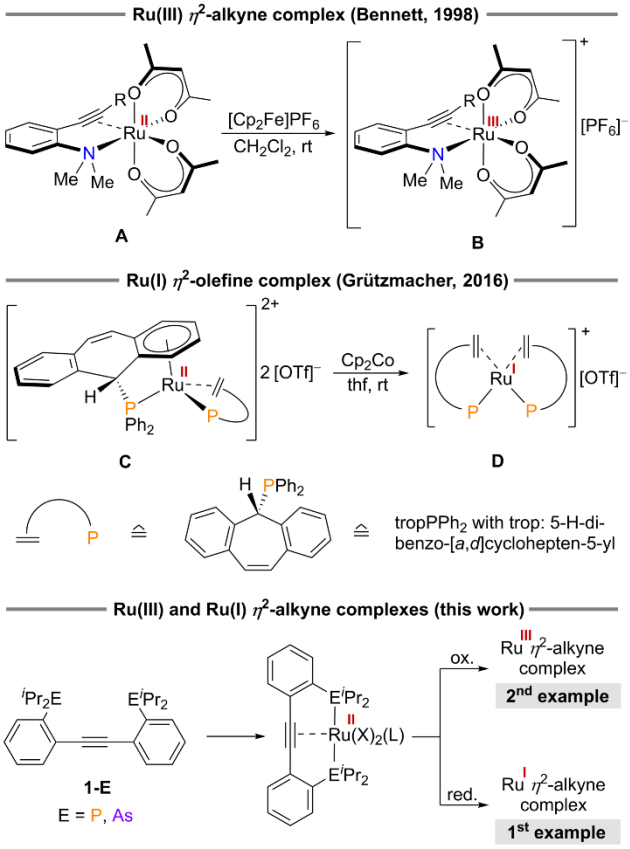

Figure 1. Bennett's Ru(III) η^2-alkyne complex (top, R = Ph, $SiMe_3$), Grützmacher's square planar Ru(I) η^2-olefin complex (middle) and our approach to Ru(III) and Ru(I) η^2-alkyne complexes (bottom).

As reported herein, several Ru(II) complexes of 1-E (E = P, As) had to be prepared at first, which turned out to be rather challenging as unexpected side-reactions and equilibria with ionic species had to be examined in detail. Once these transformations were understood, an [ECCE]-coordinated Ru(III) complex was isolated for E = As, but not for the corresponding phosphorus analog. An [ECCE]-coordinated Ru(I) complex was obtained as well, albeit for E = P only. The latter 15-valence-e^- Ru(I) η^2-alkyne complex was found to react with $TlPF_6$, which led to the formation of a trinuclear complex featuring a nearly linear Ru–Tl–Ru array. In the following, our experimental, spectroscopic and computational findings are discussed in detail.

RESULTS AND DISCUSSION

As mentioned above, 1-P was previously shown to cyclize and thus form so-called CARY-MICs (cyclic aryl ylidic mesoionic carbenes) with numerous transition metal precursors.[11] Starting from $[(\eta^6\text{-cymene})RuCl_2]_2$, 1-P and $AgSbF_6$, a CARY-MIC akin to 2-P has been isolated earlier, albeit with a $[SbF_6]^-$ counterion. Here, the corresponding chloride salt (2-P, see Scheme 1) was prepared in order to evaluate whether 2-P is prone to ring-opening to afford a pincer-type Ru(II) complex along with cymene.

Scheme 1. Synthesis of Ru(II) Complexes 2-E, 3-E and 4-E with E = P, As.

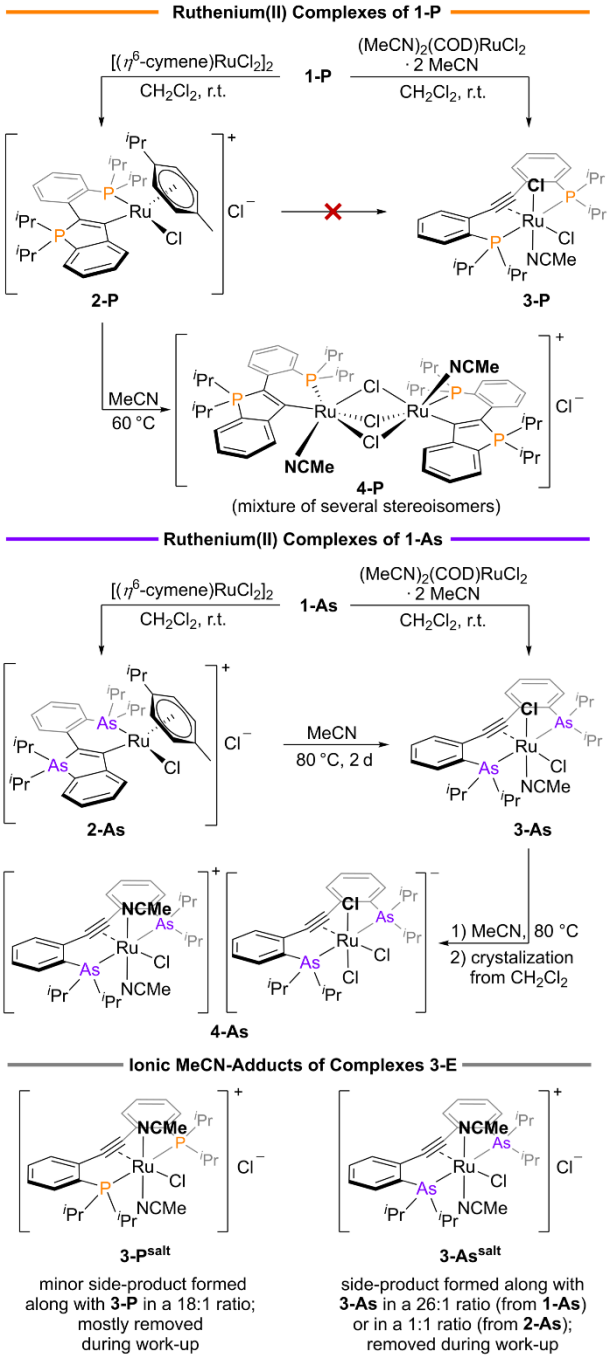

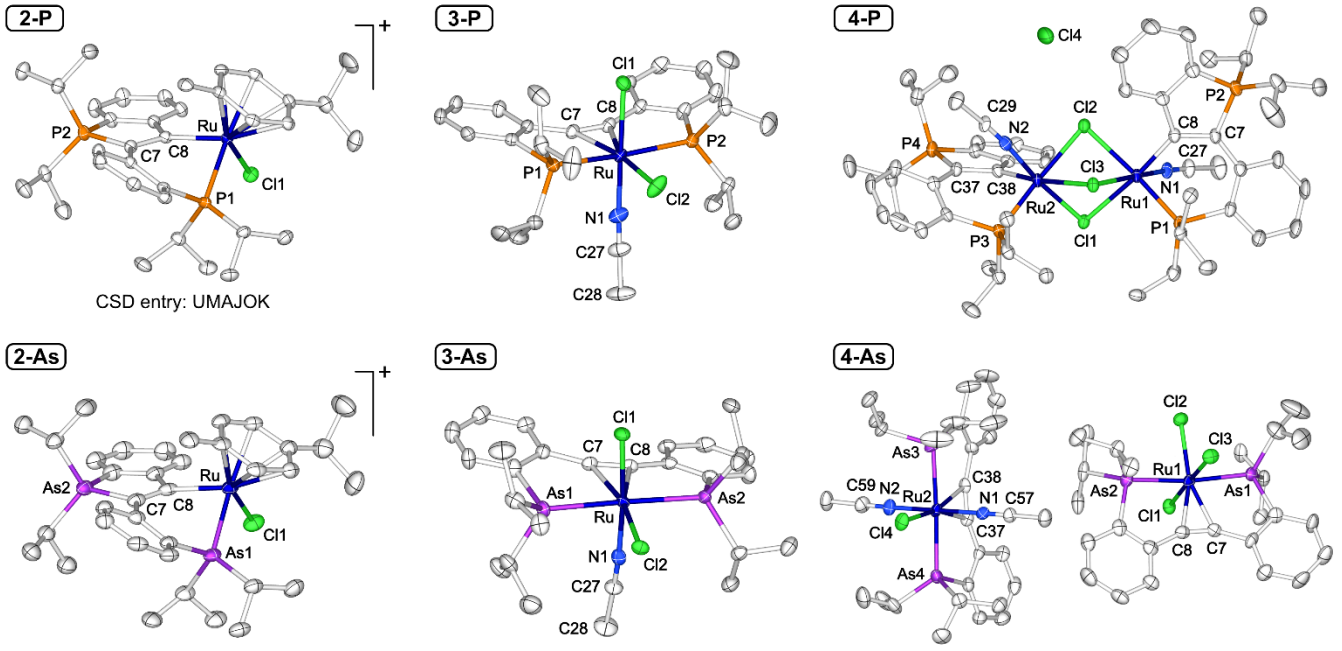

Figure 2. ORTEP plots (thermal ellipsoids set to 50% probability, co-crystallized solvents and disorder omitted for clarity) of the cation in 2-P (previously reported and shown for comparison, $[SbF_6]^-$ counterion omitted), the cation in 2-As (crystallized a triflate salt after reaction with AgOTf) and the molecular structures of 3-P, 3-As, 4-P and 4-As. Selected bond lengths (Å) and angles (°) for 2-P: Ru–P1 2.3108(5), Ru–C8 2.0669(18), Ru···centroid(cymene) 1.761913(18), C7–C8 1.387(3), P1–Ru–C8 80.77(5). Selected bond lengths (Å) and angles (°) for 2-As: Ru–As1 2.4076(5), Ru–C8 2.107(4), Ru···centroid(cymene)1.7409(15), C7–C8 1.351(6), As1–Ru–C8 80.49(10). Selected bond lengths (Å) and angles (°) for 3-P (for one out of two independent, very similar molecules in the asymmetric unit): Ru–P1 2.4144(5), Ru–P2 2.440(3), Ru–C7 2.146(2), Ru–C8 2.144(2), C7–C8 1.251(3), P1–Ru–P2 171.76(6), Cl1–Ru–Cl2 93.51(2). Selected bond lengths (Å) and angles (°) for 3-As (for one out of two independent, very similar molecules in the asymmetric unit): Ru–As1 2.4706(4), Ru–As2 2.4699(4), Ru–C7 2.159(3), Ru–C8 2.155(3), C7–C8 1.249(5), As1–Ru–As2 173.677(16), Cl1–Ru–Cl2 92.07(3). Selected bond lengths (Å) and angles (°) for 4-P: Ru1··· Ru2 3.3442(4), Ru1–P1 2.2378(15), Ru1–C8 1.998(6), Ru2–P3 2.2444(15), Ru2–C38 1.996(6), Ru1–Cl2 2.5261(14), Ru2–Cl2 2.5182(14), P1–Ru1–Cl2 175.39(5), P3–Ru2–Cl2 176.92(5), P1–Ru1··· Ru2–P3 1.77(7). Selected bond lengths (Å) and angles (°) for 4-As: Ru1–As1 2.4514(11), Ru1–As2 2.4769(11), Ru1–C7 2.133(8), Ru1–C8 2.118(8), C7–C8 1.239(12), As1–Ru1–As2 172.74(4), Cl1–Ru1–Cl3 178.45(8), Ru2–As3 2.4836(11), Ru2–As4 2.4760(11), Ru2–C37 2.185(7), Ru2–C38 2.155(8), C37–C38 1.243(12), As3–Ru2–As4 174.78(4), N1–Ru2–N2 179.7(3).

While such ring-opening reactions are known for Mo,[11] a different reactivity was noticed when 2-P was heated or irradiated in MeCN. Instead of the expected complex (3-P, see Scheme 1), three very similar complexes were formed with each of them featuring two equally intense $^{31}P\{^1H\}$ NMR signals at approximately 40 and 70 ppm.. These chemical shifts are typical for CARY-MICs,[11] while the corresponding ^1H NMR spectrum inferred that several very similar dinuclear species were produced. To confirm that dinuclear species were formed indeed, single crystals were grown from CH_2Cl_2/Et_2O and subjected to X-ray diffraction, which revealed the presence of a μ-$(Cl)_3$-bridged diruthenium(II) complex (4-P, see Scheme 1 and Figure 2).[13] Upon dissolution of these crystals, however, the aforementioned mixture of compounds was detected in the $^{31}P\{^1H\}$ NMR spectrum, suggesting that several stereoisomers of 4-P are present in solution (see SI for details). Given that pincer-type species with two spectroscopically equivalent phosphines were not detectable, an alternative synthetic route to 3-P was developed. Starting from 1-P and *cis*-$(MeCN)_2(COD)RuCl_2 \cdot 2$ MeCN, the latter target compound (3-P) was obtained, although a minor by-product (3-P^{salt}) was generated in a ratio of 3-P:3-P^{salt} = 18:1. For each compound, the expected singlet was detected in the $^{31}P\{^1H\}$ NMR spectrum at 52.1 ppm (3-P) and 54.5 ppm (3-P^{salt}), respectively. In the corresponding proton NMR spectra, a C_S- and a C_{2v}-symmetric pattern was noticed and assigned to 3-P (C_S-symmetry) and 3-P^{salt} (C_{2v}-symmetry). As expected for an ionic compound, 3-P^{salt} was found to be soluble in polar solvents (e.g. CH_2Cl_2), but nearly insoluble in benzene, while 3-P is freely soluble in benzene. These differences were then exploited to isolate 3-P in >95% purity, namely via extraction into benzene. The proposed *cis*-alignment of both chlorides in 3-P was unambiguously confirmed by single X-ray diffraction (see Figure 2). Upon heating solutions of 3-P in MeCN, neither 3-P^{salt} nor 4-P were formed, suggesting that 3-P is kinetically stable (*vide infra*).

To elucidate whether analogous [AsCCAs]-coordinated Ru(II) complexes may be prepared, $[(\eta^6$-cymene)$RuCl_2]_2$ was reacted with 1-As, which led to the formation of 2-As. This observation was actually unexpected at first given that 1-As is not susceptible to cyclization, although exceptions are known.[12b] Upon heating solutions of 2-As in MeCN to 80 °C, ring-opening was observed and 3-As was generated along with 3-As^{salt}. To suppress the formation of the latter salt, 3-As was prepared in analogy to 3-P, namely via treatment of 1-As with *cis*-$(MeCN)_2(COD)RuCl_2 \cdot 2$ MeCN at room temperature. In the latter reaction, 3-As^{salt} was generated in negligible amounts only (3-As:3-As^{salt} = 26:1) and easily removed via extraction of the target compound (3-As) into benzene. Diffusion of Et_2O into solutions of 3-As in CH_2Cl_2 led to crystalline orange plates, suited for X-ray diffraction (see Figure 2). In contrast to 3-P, pure samples of 3-

As were found to isomerize to equimolar mixtures of 3-As and 3-As^{salt} upon heating. These equimolar mixtures were also obtained via treatment of 1-As with polymeric $[(COD)RuCl_2]_x$ in MeCN at 80°C, suggesting that 3-As and 3-As^{salt} are comparable with respect to their thermodynamic stabilities. In an attempt to also grow single crystals of 3-As^{salt}, a solution of 3-As in MeCN was partially isomerized to 3-As^{salt} at 80 °C. Upon crystallization of the thus obtained mixture from CH_2Cl_2, dark green crystals were obtained and identified as 4-As (see Scheme 1) by single crystal X-ray diffraction. In the molecular structure of 4-As, a *trans*-{[AsCCAs]RuCl(MeCN)$_2$}$^+$ cation and an {[AsCCAs]RuCl$_3$}$^-$ anion were found with each ruthenium in the +II oxidation state (see Figure 2). Samples of 4-As in CD_2Cl_2 were found to exhibit well-resolved ^{1}H NMR signals for the cation and broad signals for the anion, even at −80°C. Upon dissolution of crystalline 4-As in MeCN, a nearly equimolar mixture of 3-As^{salt} and 3-As was formed, suggesting that MeCN reacts with the anion in 4-As to produce 3-As in addition to a chloride ion, which then serves as a counterion for {[AsCCAs]RuCl(MeCN)$_2$}$^+$ to thus produce 3-As^{salt}. Given that the latter reaction was found to occur instantaneously, it is inferred that 4-As is not only kinetically but also thermodynamic less stable (*vide infra*) than 3-As and 3-As^{salt}, at least in the presence of MeCN.

To gauge the different thermodynamic stabilities of 2-E, 3-E, 3-E^{salt} (E = P, As) and their "bimetallic" salts 4-P and 4-As, DFT-modelling studies were carried out on the PBE0/def2-TZVP (D3BJ, CPCM for MeCN)[14] level of theory. For comparison, compounds 2-E were set to 0.0 kcal/mol and the relative Gibbs free energies of 3-E, 3-E^{salt} and 4-E were calculated taking the leaving cymene and incoming MeCN ligand(s) into account. As shown in Figure 3, each 3-E/3-E^{salt} pair is energetically nearly degenerate, while drastic differences are evident upon comparison of each pair to the corresponding CARY-MIC complexes 2-E. For E = P, the 3-P/3-P^{salt} pair is only slightly more stable than 2-P, while a stabilization of 13.7 kcal/mol was calculated for 3-As relative to 2-As. This finding is in line with the experimental observation that 2-As may be converted to 3-As, which is not the case for E = P as different stereoisomers of 4-P are formed preferably upon heating of 2-P in MeCN. This finding is also reflected by our DFT analysis given that an exergonic reaction was calculated for the conversion of 2-P to 4-P. Along these lines, several stereoisomers of 4-P were examined *in silico*, which revealed that the crystallographically characterized isomer (4-P) is the most stable one (see SI for details).

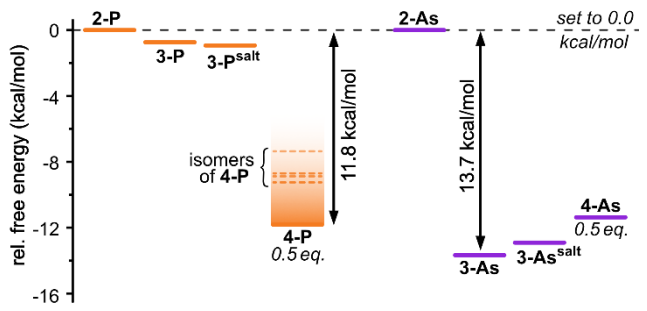

Figure 3. Comparison of the thermodynamic stabilities of 3-E, 3-E^{salt} and 4-E relative to 2-E (set to 0.0 kcal/mol) with E = P, As. The Gibbs free energies for each compound were computed on the PBE0/def2-TZVP (D3BJ, CPCM for MeCN) level of theory and corrected for leaving and incoming ligands (see SI for details).

For 4-As, a different situation was encountered in our experiments given that 4-As was found to readily disassemble to 3-As and 3-As^{salt} upon dissolution in MeCN. This observation is in line with our DFT analysis, which revealed that 4-As is thermodynamically disfavored by approximately 3 kcal/mol relative to the most stable [AsCCAs]-coordinated Ru(II) complex 3-As (see Figure 3). Despite the good agreement between the computational and experimental findings, a cautious note is mandatory given that our analysis refers to the thermodynamic stabilities only. While 4-P was found to be the thermodynamically most stable ruthenium(II) complex within the series of *P*-containing complexes, 3-P and 3-P^{salt} seem to be kinetically stabilized products, given that neither 3-P nor 3-P^{salt} were converted to 4-P upon heating. Hence, the presence of at least one energetically high-lying transition state, which interferes with this (otherwise reasonable) conversion, is suggested on basis of our experimental observations.

With compounds 3-E (E = P, As) available, trichloro ruthenium(III) complexes were targeted via 1e$^-$ oxidation[15] of 3-E using $PhICl_2$ as a convenient synthon for chlorine gas. Monitoring the latter conversions by ^{1}H NMR spectroscopy revealed that several unidentified diamagnetic products were generated predominantly, although broad paramagnetically shifted resonances indicative of Ru(III) species were observed as well. While these Ru(III) species were actually identified (*vide infra*) as the desired [ECCE]RuCl$_3$ derivatives (7-E, see Scheme 2), clean samples were not obtained, although numerous attempts to optimize these conversions were made. Hence, we decided to replace the MeCN co-ligands in 3-E for CO and oxidize the resulting complexes in a subsequent step. While the envisioned carbonyl complexes 5-E were obtained without difficulties (see Scheme 2), no paramagnetic Ru(III) species were formed upon reaction of 5-E with $PhICl_2$. Instead, diamagnetic oxidation products were isolated in each case (E = P, As) and identified as compounds 6-E (see Scheme 2).

Scheme 2. Synthesis of 6-E and 7-As via Oxidation of 5-E and 8, respectively.

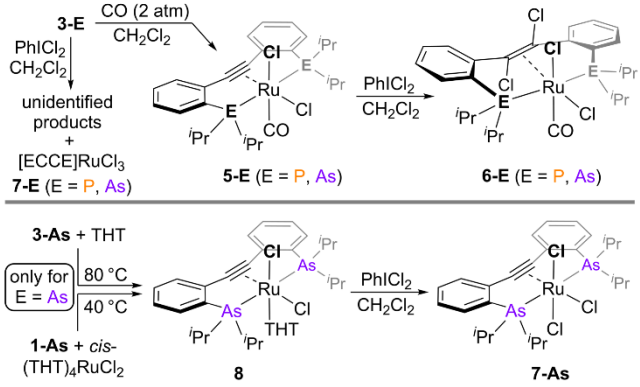

In the latter reactions, the alkyne unit within each ligand backbone was chlorinated in a *trans*-selective manner, which led to the consumption of one equivalent of $PhICl_2$, while incomplete conversions were noticed with sub-stoichiometric amounts of $PhICl_2$. The crystallographically determined molecular structures of 5-E and 6-E (see SI for E = P, see Figure 4 for E = As) confirmed that the Ru-bound chlorides in 5-E and 6-E are *cis*-configured in each case, while the carbon-bound chlorides in 6-E are *trans*-configured. NMR and

IR spectroscopic data for each complex ($\tilde{\nu}_{CO}$ = 1948 cm^{-1} for 5-P, 1943 cm^{-1} for 5-As, 1999 cm^{-1} for 6-P, 1991 cm^{-1} for 6-As) are in line with the latter structures and suggests that the extent of π-backbonding $4d$(Ru)→π^*(CO) decreases during the conversion of 5-E to 6-E. Assuming that the different reactivities of 5-E and 3-E (upon oxidation with $PhICl_2$) are related to the different π-acceptor characteristics of the co-ligands (CO *vs.* MeCN), we speculated that co-ligands with a further diminished π-acceptor character (such as THT) may favor metal-centered oxidation events. Hence, attempts to replace the MeCN co-ligands in 3-E for THT were made, but the desired THT-adduct 8 was only obtained in the case of 3-As, while numerous unidentified product were generated upon treatment of 3-P with THT. Interestingly, 8 is also obtained starting from *cis*-$(THT)_4RuCl_2$ and 1-As, while the analogous reaction once again failed for the phosphorus derivative 1-P.

Starting from 8 and $PhICl_2$, the envisioned ruthenium(III) trichloride 7-As was produced in a fairly clean reaction and isolated in the form of nearly black crystals in 55% yield (see Scheme 2). In the ^{1}H NMR spectrum of 7-As, characteristic signals were detected at 16.60, −1.30, −1.76 and −8.92 ppm, which confirmed that 7-As was also formed upon oxidation of 3-As, albeit unselectively (*vide supra*).[16] In the X-band EPR spectrum of 7-As (r.t., 2-Me-thf), only one broad signal was detected at g = 2.09 (see Figure 4), which further broadened upon cooling to 4 K (see SI for details). Despite the fact that the principle g-components (g_1, g_2, g_3) were unresolved at 4 K, the presence of a metal-centered radical is proposed due to the aforementioned line broadening of the signal and its significant low-field shift relative to the g-value for a free electron (g_e = 2.0023). To corroborate the latter proposal, spin-unrestricted DFT calculations were carried out at the ZORA-PBE0/def2-TZVP level of theory including all electrons.[14a, e, 17] These calculations revealed that the unpaired electron in 7-As is mainly localized at the Ru(III) core (Mulliken spin population = +0.83), while delocalization to the alkyne moiety is of minor importance (Mulliken spin population at each alkyne carbon atom = +0.05). CASSCF(9,9) calculations (active space: $\pi_{||}$(alkyne), $\pi_{\perp}$(alkyne), $\pi_{||}$*(alkyne), $\pi_{\perp}$*(alkyne) and five d-orbitals with overall 9 e^-) confirmed this interpretation and suggested that the unpaired electron is located in one of the "t_{2g}-type" orbitals (d_{xy}, d_{xz} or d_{yz} depending on the orientation of the coordinate system, see SI for details).

In comparison to the {[AsCCAs]$RuCl_3$}$^-$ anion in 4-As (Ru–C = 2.133(8) and 2.118(8) Å), slightly contracted Ru–C distances have been found in 7-As (Ru–C = 2.084(2) Å each), while the C≡C bonds are actually *not* significantly different (3σ condition, anion in 4-As: $d_{C\equiv C}$ = 1.239(12) Å, 7-As: $d_{C\equiv C}$ = 1.265(4) Å). A nearly identical observation has been made upon comparison of A and B (*cf.* Figure 1) and it was speculated that the electron removed upon oxidation originates from an antibonding Ru-alkyne HOMO in A, which comprises the $\pi_{\perp}$(alkyne) and a filled $4d$(Ru) orbital.[6] An inspection of the HOMO in {[AsCCAs]$RuCl_3$}$^-$ and the SOMO in 7-As is in line with this proposal, although the oxidation is predominately metal-centered (*cf.* Mulliken spin population in 7-As), which may explain that the apparent lengthening of the C≡C bond is actually within the experimental error.

With the second example of a comparable pair of Ru(II) and Ru(III) η^2-alkyne complexes well characterized, we turned our attention to the preparation of a hitherto unprecedented Ru(I) η^2-alkyne derivative. In an extensive screening, compounds 3-E (E = P, As) were treated with different reductants (e.g. KC_8, Na/Pb, Mashima's salt-free reductant or Rieke-Zn). For all these reductants, a color change

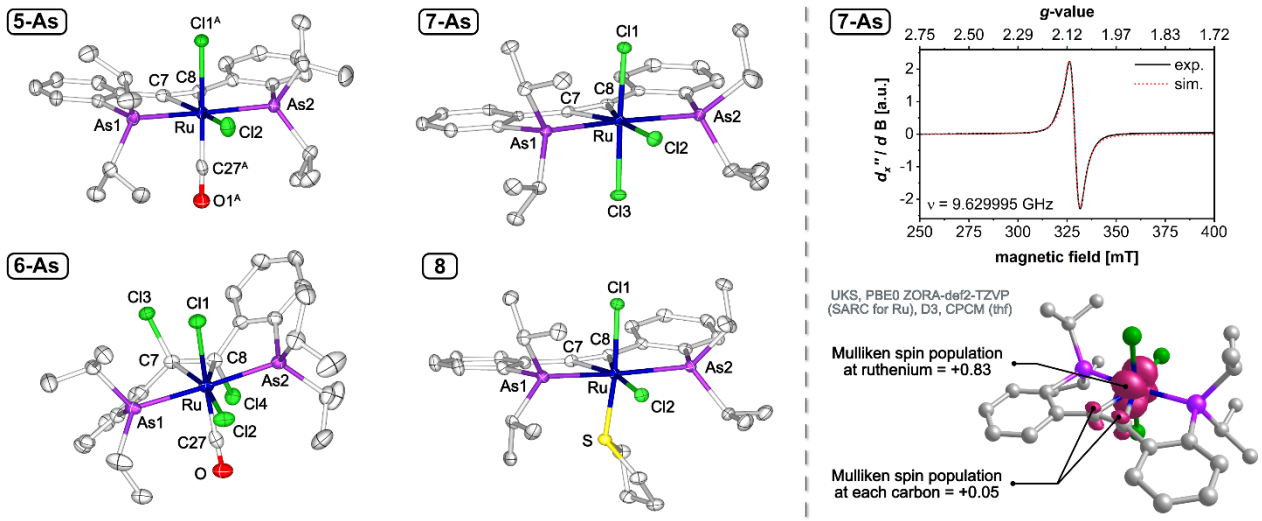

Figure 4. Left: ORTEP plots (thermal ellipsoids set to 50% probability, co-crystallized solvents and disorder omitted for clarity) of the molecular structures of 5-As, 6-As, 7-As and 8. Selected bond lengths (Å) and angles (°) for 5-As: Ru–As1 2.4763(5), Ru–As2 2.4675(4), Ru–C7 2.182(3), Ru–C8 2.182(3), C7–C8 1.246(5), As1–Ru–As2 171.819(17), $C27^A$–Ru–$Cl1^A$ 179.46(14). Selected bond lengths (Å) and angles (°) for 6-As: Ru–As1 2.5022(8), Ru–As2 2.4907(8), Ru–C7 2.219(6), Ru–C8 2.186(6), C7–C8 1.409(9), As1–Ru–As2 170.39(3), C27–Ru–Cl1 173.4(2). Selected bond lengths (Å) and angles (°) for 7-As: Ru–As1 2.4783(3), Ru–As2 2.5134(3), Ru–C7 2.084(2), Ru–C8 2.084(2), C7–C8 1.265(4), As1–Ru–As2 172.727(12), Cl1–Ru–Cl3 177.50(2). Selected bond lengths (Å) and angles (°) for 8 (for one out of two independent, very similar molecules in the asymmetric unit): Ru–As1 2.4773(3), Ru–As2 2.4785(3), Ru–C7 2.156(2), Ru–C8 2.158(2), C7–C8 1.254(3), As1–Ru–As2 171.883(10), S–Ru–Cl1 173.577(19). Right: Isotropic X-band EPR spectrum of 7-As (r.t., 2-Me-thf, modulation frequency = 100.0 kHz, microwave power = 0.1257 mW, modulation amplitude = 5.0 G) together with the calculated spin densities of 7-As.

from red to deep green was observed and the reaction with Mashima's reductant was found to be fairly clean for E = P according to ^{1}H NMR spectroscopy (*vide infra*). For E = As, however, the green color was only visible in the presence of excess reductant, but faded upon consumption or removal of the reductant. Assuming that this observation is related to decomposition of the reduced Ru(I) species in case of E = As, the focus was set on the isolation of the phosphorus derivative, also as all our attempts to isolate the *arsa*-derivative at lower temperatures were unsuccessful. For E = P, however, the envisioned reduced Ru(I) complex (**9**, see Scheme 3) was readily obtained in 51% yield after crystallization from Et_2O at −40 °C.

Scheme 3. Synthesis of 9 and 10.

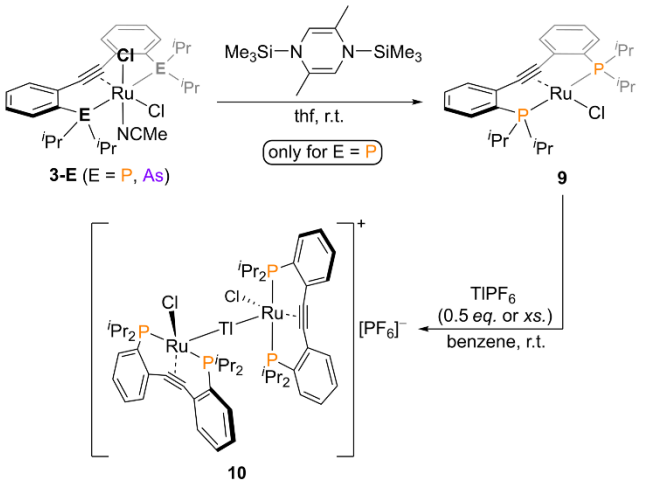

The structure of **9** was elucidated by single crystal X-ray diffraction, which confirmed the presence of a square planar ruthenium(I) complex (see Figure 5). The alkyne C≡C bond in **9** (1.272(7) Å) is slightly elongated in comparison to 3-P (1.251(3) Å), while shorter Ru–C distances are evident in **9**, suggesting that the alkyne in **9** is more strongly bound than the alkyne in 3-P. This observation, however, cannot be interpreted in more depth as different coordination polyhedra are present in **9** and 3-P (square planar *vs.* octahedral). In the ^{1}H NMR spectrum of **9**, overall seven broad signals were detected and tentatively assigned to the diastereotopic ^{i}Pr-methyl groups and the ^{i}Pr-CH or aryl protons on basis of their relative integrals. At room temperature, no EPR signal was detectable, but a magnetic moment of μ_{eff} = 1.58 μ_B was determined (C_6D_6, r.t., Evans method[18]), indicative of one unpaired electron. In frozen 2-Me-thf at 4 K, an axial EPR pattern was found and simulated with g_1 = 2.859, g_2 = 1.916 and g_3 = 1.910 (see Figure 5). The pronounced anisotropy of the latter EPR signal is in line with the presence of a square planar complex and a metal-centered radical. To further elucidate the electronic situation in **9**, multireference calculation were carried out on the ZORA-PBE0/def2-TZVP level of theory.[14a, e, 17] On basis of QD-NEVPT2/CASSCF(11,9) calculations (active space: $\pi_{||}$(alkyne), $\pi_{\perp}$(alkyne), $\pi_{||}$*(alkyne), $\pi_{\perp}$*(alkyne) and five *d*-orbitals with overall 11 e^-), it became clear that the SOMO is predominantly metal-centered, while CSFs (configuration state functions) resulting from π-donation ($\pi_{\perp}$ to d_{yz}) and δ-backdonation (d_{xz} to $\pi_{\perp}$*) were found to play a minor role (see SI for details). Hence, the alkyne is interpreted as a 2e^- donor, rendering **9** a 15-valence e^- species akin to Grützmacher's square planar Ru(I) complex **D** (*cf.* Figure 1). Truncation of the active space to solely included the *d*-orbitals led to a state-averaged QD-NEVPT2-corrected CASSCF(7,5) solution (averaged over all 40 doublet and 10 quartet CSFs), which was used for a subsequent AILFT (ab initio ligand field theory) analysis.[19] This analysis confirmed the doublet ground state of **9** with a dominating contribution (86%) resulting from a $(d_{xy})^2(d_{xz})^2(d_{z^2})^2(d_{yz})^1(d_{x^2-y^2})^0$ configuration and a minor contribution (11%) resulting from a $(d_{xy})^2(d_{xz})^2(d_{z^2})^1(d_{yz})^2(d_{x^2-y^2})^0$ configuration (z-axis perpendicular the coordination plane, see Figure 5).

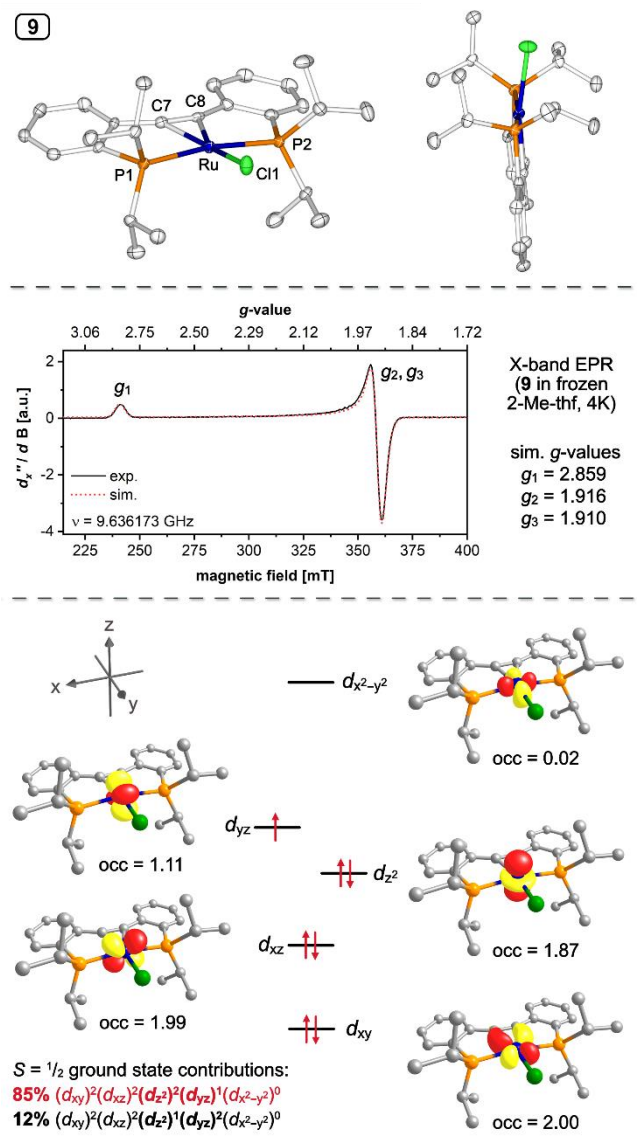

Figure 5. Top: ORTEP plot (thermal ellipsoids set to 50% probability) of the molecular structure of **9**. Selected bond lengths (Å) and angles (°) for **9** (for one out of two independent, very similar molecules in the asymmetric unit: Ru–P1 2.3635(13), Ru–P2 2.3567(12), Ru–C7 2.038(5), Ru–C8 2.039(5), C7–C8 1.272(7), P1–Ru–P2 170.78(5). Middle: X-band EPR spectrum of **9** (4 K, 2-Me-thf, modulation frequency = 100.0 kHz, microwave power = 0.6293 mW, modulation amplitude = 1.0 G). Bottom: AIFLT analysis for **9** (carried out on top of a state-averaged QD-NEVPT2-corrected CASSCF(7,5) calculation, see text, see SI for technical details).

The latter ligand field splitting diagram strongly suggested that the coordination of axial co-ligands (to form octahedral derivatives of **9**)

is actually impossible due to absence of an empty d_{z^2} orbital. Indeed, no reaction was observed with thf, MeCN or PMe_3, while vast decomposition set in immediately upon addition of CO. In an attempt to remove the chloride in 9 to gain access to the unoccupied $d_{x^2-y^2}$ orbital, 9 was reacted with excess $TlPF_6$. To our surprise, only half an equivalent of $TlPF_6$ was consumed and a single diamagnetic compound was generated. No precipitate of TlCl was noticed, while the reaction product was freely soluble in CH_2Cl_2, suggesting that (*i*) the chloride in 9 was still in place and that (*ii*) a molecular species was generated rather than a coordination polymer.[20] In the ^{1}H NMR spectrum, two sets of signals for two distinct ligands were found, which has been previously observed for dimers with two mutually twisted halves. In the ^{31}P NMR spectrum, a septet (indicative of a $[PF_6]^-$ counterion) was found in addition to two broad signals for the ligands' phosphines. These data strongly inferred that two molecules of 9 dimerized via a central Tl-bridge to produce compound 10 (see Scheme 3). To confirm this assignment, single crystals suitable for X-ray diffraction were grown via diffusion of pentane into a solution of 10 in CH_2Cl_2. In the cation of 10, two μ-Tl-bridged {[PCCP]RuCl} units were found to form a nearly linear Ru–Tl–Ru array ($\measuredangle_{Ru-Tl-Ru}$ = 172.732(13)°) with Ru–Tl distances of 2.5634(3) and 2.5572(4) Å, respectively. The P–Ru–P vectors in each {[PCCP]RuCl} moiety are mutually twisted by 73.97(3)° with each Ru atom slightly deflected out of its [PCCP] plane towards the central Tl atom (see Figure 6). Interestingly, structurally related compounds with similar Ru–Tl–Ru motifs, such as $[\{CpRu(dppe)\}_2(\mu\text{-}Tl)][PF_6]$ or $[\{CpRu(CO)_2\}_2(\mu\text{-}Tl)][BF_4]$ have been reported previously.[21] In the latter case, the Ru–Tl–Ru bonding interaction was examined and it was suggested that $[\{CpRu(CO)_2\}_2(\mu\text{-}Tl)]^+$ is "best represented as Ru^0–Tl^I–Ru^0" (which *formally* does not add up in our opinion). Despite the confusion regarding the formal oxidation states, a detailed QTAIM analysis[22] for $[\{CpRu(CO)_2\}_2(\mu\text{-}Tl)]^+$ revealed the presence of (3, −1) bond critical points close to the midpoints of each Ru–Tl bond with ρ_{bcp} = 0.065 eÅ^{-3} and $\nabla^2(\rho_{bcp})$ = 0.12 eÅ^{-6}. In the case of 10,[23] very similar bond critical point with similar values for the electron densities ρ_{bcp} and Laplacians of the electrons densities $\nabla^2(\rho_{bcp})$ were found as summarized in Figure 6. These values may either be interpreted in terms of an ionic interaction or in terms of a 3*c*-4*e*$^-$ bond.[24] For the 3*c*-4*e*$^-$ bond in $[Cl_3]^-$, for example, electron densities of ρ_{bcp} = 0.063 eÅ^{-3} and Laplacians of $\nabla^2(\rho_{bcp})$ = 0.117 eÅ^{-6} were determined for both bond critical points.[25] To evaluate whether our QTAIM analysis is in line with the presence of a 3*c*-4*e*$^-$ bond in 10, the delocalization index δ, which is related to the total number of *electron pairs* shared between two atoms,[26] was calculated suggesting that overall 4 electrons are shared across the Ru–Tl–Ru unit ($\delta_{Ru-Tl-Ru}$ = 0.94 + 0.95 ≈ 2 electron pairs). A Wiberg bond index (WBI) of approximately 0.4 was determined for each Ru–Tl bond via NBO analysis, which infers the presence of one *bonding electron pair* delocalized over the Ru–Tl–Ru unit. Taken together, these findings are interpreted in terms of a typical 3*c*-4*e*$^-$ with 2 bonding and 2 non-bonding electrons.[27] Inspection of the intrinsic bond orbitals (IBOs), which are exact representations of the molecular Kohn-Sham wavefunctions,[28] further confirmed this interpretation and suggested the presence of a bonding, a nonbonding and a antibonding interaction between two Ru 4d_{z^2} orbitals and one Tl 6s orbital (see Figure 6). The bonding (no nodal plane) and the non-bonding orbitals (one nodal plane) were both found to be doubly occupied, while the anti-bonding orbital (two nodal planes) was found to be unoccupied. On basis of this simplified picture, a bond order of 0.5 (cf. WBI = 0.4) is proposed for each Ru–Tl bond.

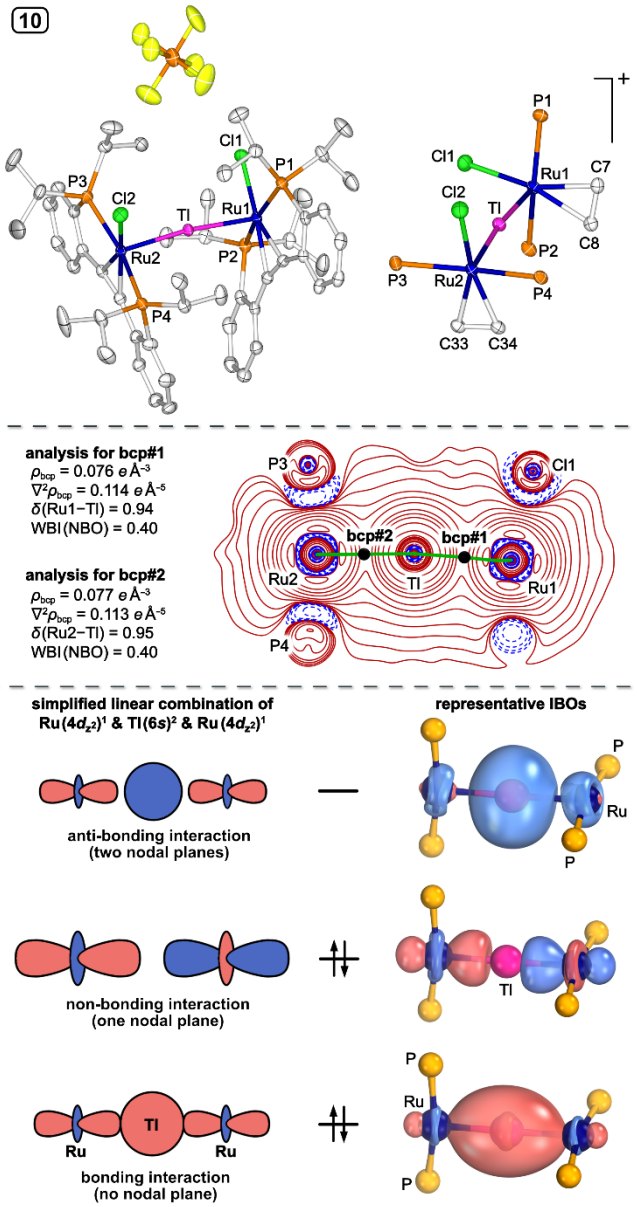

Figure 6. Top: ORTEP plot (thermal ellipsoids set to 50% probability) of the molecular structure of 10 (co-crystallized CH_2Cl_2 and positional CH_2Cl_2/$[PF_6]^-$ disorder omitted for clarity). Selected bond lengths (Å) and angles (°) for 10: Ru1–Tl 2.5634(3), Ru2–Tl 2.5572(4), Ru1–P1 2.3765(12), Ru1–P2 2.3799(12), Ru1–C7 2.116(4), Ru1–C8 2.105(4), Ru2–P3 2.3879(11), Ru2–P4 2.3813(12), Ru2–C33 2.101(4), Ru2–C34 2.098(4), C7–C8 1.264(6), C33–C34 1.261(6), Ru1–Tl–Ru2 172.732(13), P1–Ru1–P2 164.82(4), P3–Ru2–P4 166.17(4), P1···P2···P3···P4 73.97(3). Middle: Plot of $\nabla^2\rho(r)$ for the cation in 10 along a plane containing the Tl and both Ru nuclei. Red contour lines indicate regions with charge depletion ($\nabla^2\rho(r) > 0$) and blue (dashed) contour lines indicate regions with charge accumulation ($\nabla^2\rho(r) < 0$). Selected bond paths and (3,–1) bond critical points (bcp#1 and bcp#2) are shown as green lines and black circles, respectively. Bottom: Schematic illustration of the 3*c*-4*e*$^-$ bonding situation in 10 together with representative IBOs.

CONCLUSIONS

In summary, a variety of ruthenium(II) complexes bearing ligands 1-E (E = P, As) have been prepared, which - *inter alia* - demonstrated that the partially cyclized complexes 2-E are prone to ring-opening for E = As. Given that this reaction was not observed for E = P, alternative synthetic routes to complexes of the type [ECCE]$RuCl_2$(L) with L = MeCN (3-E) and L = CO (5-E) were developed for E = P and for E = As, while the closely related tetrahydrothiophene adduct (L = THT) was obtained for E = As (8) only. Upon oxidation of 8 with $PhICl_2$, [AsCCAs]$RuCl_3$ (7-As) was obtained and shown to exhibit a slightly strengthened Ru(III) alkyne interaction in comparison to the corresponding Ru(II) anion {[AsCCAs]$RuCl_3$}$^-$. Reduction of 3-P led to the isolation of the first Ru(I) η^2-alkyne complex 9. This square planar 15-valence-e^- Ru(I) species was found to cleanly react with $TlPF_6$ to afford a μ-Tl bridged diruthenium complex (10) featuring a 3*c*-4e^- Ru–Tl–Ru bond.

ASSOCIATED CONTENT

Supporting Information

The Supporting Information is available free of charge.
Experimental procedures, selected spectroscopic data, computational details and crystallographic data (PDF)
Optimized coordinates for all new compounds (XYZ)

AUTHOR INFORMATION

Corresponding Author

Joachim Ballmann, E-mail: joachim.ballmann@uni-heidelberg.de

ORCID

Joachim Ballmann: 0000-0001-6431-4197

Notes

The authors declare no competing financial interest.

ACKNOWLEDGMENT

Funding from the DFG (BA 4859/3-1) and support by the state of Baden-Württemberg through bwHPC and the DFG through grant number INST 40/575-1 FUGG (JUSTUS 2 cluster) is gratefully acknowledged. We thank Prof. L. H. Gade for generous support and continued interest in our work.

REFERENCES

(1) (a) Trost, B. M.; Ball, Z. T. Markovnikov Alkyne Hydrosilylation Catalyzed by Ruthenium Complexes. *J. Am. Chem. Soc.* 2001, *123*, 12726-12727; (b) Arockiam, P. B.; Bruneau, C.; Dixneuf, P. H. Ruthenium(II)-Catalyzed C–H Bond Activation and Functionalization. *Chem. Rev.* 2012, *112*, 5879-5918; (c) Sundararaju, B.; Fürstner, A. A trans-Selective Hydroboration of Internal Alkynes. *Angew. Chem. Int. Ed.* 2013, *52*, 14050-14054; (d) Ackermann, L. Carboxylate-Assisted Ruthenium-Catalyzed Alkyne Annulations by C–H/Het–H Bond Functionalizations. *Acc. Chem. Res.* 2014, *47*, 281-295; (e) Rummelt, S. M.; Fürstner, A. Ruthenium-Catalyzed trans-Selective Hydrostannation of Alkynes. *Angew. Chem. Int. Ed.* 2014, *53*, 3626-3630; (f) Roşca, D.-A.; Radkowski, K.; Wolf, L. M.; Wagh, M.; Goddard, R.; Thiel, W.; Fürstner, A. Ruthenium-Catalyzed Alkyne *trans*-Hydrometalation: Mechanistic Insights and Preparative Implications. *J. Am. Chem. Soc.* 2017, *139*, 2443-2455; (g) Duarah, G.; Kaishap, P. P.; Begum, T.; Gogoi, S. Recent Advances in Ruthenium(II)-Catalyzed C–H Bond Activation and Alkyne Annulation Reactions. *Adv. Synth. Catal.* 2019, *361*, 654-672; (h) Park, S. H.; Wang, S.-G.; Cramer, N. Enantioselective Ruthenium(II)-Catalyzed Access to Benzonorcaradienes by Coupling of Oxabenzonorbornadienes and Alkynes. *ACS Catal.* 2019, *9*, 10226-10231.

(2) Chatani, N. Product Class 8: Organometallic Complexes of Ruthenium. In *Science of Synthesis, Category 1, Organometallics*; Lautens, M. (Ed.); Georg Thieme Verlag KG, 2001; pp 931-972.

(3) (a) Dixneuf, P. H. Activation of alkynes with ruthenium complexes. *Pure Appl. Chem.* 1989, *61*, 1763-1770; (b) Comas-Vives, A.; Ujaque, G.; Lledós, A. Theoretical Analysis of the Hydrogen-Transfer Reaction to C═N, C═C, and C≡C Bonds Catalyzed by Shvo's Ruthenium Complex. *Organometallics* 2008, *27*, 4854-4863; (c) McInturff, E. L.; Nguyen, K. D.; Krische, M. J. Redox-Triggered C–C Coupling of Diols and Alkynes: Synthesis of β,γ-Unsaturated α-Hydroxyketones and Furans by Ruthenium-Catalyzed Hydrohydroxyalkylation. *Angew. Chem. Int. Ed.* 2014, *53*, 3232-3235; (d) Hu, F.; Szostak, M. Ruthenium(0)-catalyzed hydroarylation of alkynes via ketone-directed C–H functionalization using in situ-generated ruthenium complexes. *Chem. Commun.* 2016, *52*, 9715-9718; (e) Luong, T.; Chen, S.; Qu, K.; McInturff, E. L.; Krische, M. J. Ruthenium(0)-Catalyzed C–C Coupling of Alkynes and 3-Hydroxy-2-oxindoles: Direct C–H Vinylation of Alcohols. *Org. Lett.* 2017, *19*, 966-968.

(4) Whittlesey, M. K. Mononuclear Ru/Os Compounds with Hydrocarbon Ligands: Compounds with η^1-Ligands. In *Comprehensive Organometallic Chemistry III*, Mingos, D. M. P., Crabtree, R. H. (Eds.); Elsevier, 2007; pp 385-440.

(5) Ru(I) and Ru(III) species have been proposed to play a role in catalysis, in particualr in C–H activation reactions. For Ru(I), see: Li, Z.-Y.; Li, L.; Li, Q.-L.; Jing, K.; Xu, H.; Wang, G.-W. Ruthenium-Catalyzed meta-Selective C–H Mono- and Difluoromethylation of Arenes through ortho-Metalation Strategy. *Chem. – Eur. J.* 2017, *23*, 3285-3290. For Ru(III), see: (a) Li, J.; Warratz, S.; Zell, D.; De Sarkar, S.; Ishikawa, E. E.; Ackermann, L. N-Acyl Amino Acid Ligands for Ruthenium(II)-Catalyzed meta-C–H *tert*-Alkylation with Removable Auxiliaries. *J. Am. Chem. Soc.* 2015, *137*, 13894-13901; (b) Paterson, A. J.; St John-Campbell, S.; Mahon, M. F.; Press, N. J.; Frost, C. G. Catalytic meta-selective C–H functionalization to construct quaternary carbon centres. *Chem. Commun.* 2015, *51*, 12807-12810; (c) Leitch, J. A.; Frost, C. G. Ruthenium-catalysed σ-activation for remote meta-selective C–H functionalisation. *Chem. Soc. Rev.* 2017, *46*, 7145-7153; (d) Korvorapun, K.; Kaplaneris, N.; Rogge, T.; Warratz, S.; Stückl, A. C.; Ackermann, L. Sequential *meta*-/*ortho*-C–H Functionalizations by One-Pot Ruthenium(II/III) Catalysis. *ACS Catal.* 2018, *8*, 886-892; (e) Liu, H.-C.; Kong, X.; Gong, X.-P.; Li, Y.; Niu, Z.-J.; Gou, X.-Y.; Li, X.-S.; Wang, Y.-Z.; Shi, W.-Y.; Huang, Y.-C.; Liu, X.-Y.; Liang, Y.-M. Site-selective coupling of remote C(sp^3)–H/*meta*-C(sp^2)–H bonds enabled by Ru/photoredox dual catalysis and mechanistic studies. *Chem. Sci.* 2022, *13*, 5382-5389; (f) Chen, X.; Gülen, H. C.; Wu, J.; Zhang, Z.-J.; Hong, X.; Ackermann, L. Close-Shell Reductive Elimination versus Open-Shell Radical Coupling for Site-Selective Ruthenium-Catalyzed C–H Activations by Computation and Experiments. *Angew. Chem. Int. Ed.* 2023, *62*, e202302021.

(6) Bennett, M. A.; Heath, G. A.; Hockless, D. C. R.; Kovacik, I.; Willis, A. C. Chelate Alkyne Complexes of Divalent and Trivalent Ruthenium Stabilized by *N*-Donor Ligation. *Organometallics* 1998, *17*, 5867-5873.

(7) Bennett, M. A.; Heath, G. A.; Hockless, D. C. R.; Kovacik, I.; Willis, A. C. Alkene Complexes of Divalent and Trivalent Ruthenium Stabilized by Chelation. Dependence of Coordinated Alkene Orientation on Metal Oxidation State. *J. Am. Chem. Soc.* 1998, *120*, 932-941.

(8) (a) Federmann, P.; Richter, T.; Wadepohl, H.; Ballmann, J. Synthesis and Reactivity of [PCCP]-Coordinated Group 5 Alkyl and Alkylidene Complexes Featuring a Metallacyclopropene Backbone. *Organometallics* 2019, *38*, 4307-4318; (b) Wagner, H. K.; Ansmann, N.; Gentner, T.; Wadepohl, H.; Ballmann, J. The Multifaceted Palladium Chemistry of 2,2′-Diphosphinotolanes. *Organometallics* 2021, *40*, 804-812.

(9) (a) Takaoka, A.; Gerber, L. C. H.; Peters, J. C. Access to Well-Defined Ruthenium(I) and Osmium(I) Metalloradicals. *Angew. Chem. Int. Ed.* 2010, *49*, 4088-4091; (b) Poli, R. Ruthenium and Osmium Metalloradicals. *Angew. Chem. Int. Ed.* 2011, *50*, 43-45; (c) Gilbert-Wilson, R.; Field, L. D.; Colbran, S. B.; Bhadbhade, M. M. Low Oxidation State Iron(0), Iron(I), and

Ruthenium(0) Dinitrogen Complexes with a Very Bulky Neutral Phosphine Ligand. *Inorg. Chem.* 2013, *52*, 3043-3053; (d) Yang, X.; Gianetti, T. L.; Harbort, J.; Wörle, M. D.; Tan, L.; Su, C.-Y.; Jurt, P.; Harmer, J. R.; Grützmacher, H. From 0 to II in One-Electron Steps: A Series of Ruthenium Complexes Supported by TropPPh$_2$. *Angew. Chem. Int. Ed.* 2016, *55*, 11999-12002; (e) van de Watering, F. F.; van der Vlugt, J. I.; Dzik, W. I.; de Bruin, B.; Reek, J. N. H. Metalloradical Reactivity of Ru^{I} and Ru^{0} Stabilized by an Indole-Based Tripodal Tetraphosphine Ligand. *Chem. – Eur. J.* 2017, *23*, 12709-12713.

(10) (a) Sherlock, S. J.; Boyd, D. C.; Moasser, B.; Gladfelter, W. L. Homogeneous catalytic carbonylation of nitroaromatics. 4. Preparation and characterization of ruthenium radical cations. *Inorg. Chem.* 1991, *30*, 3626-3632; (b) Bianchini, C.; Peuzzini, M.; Ceccanti, A.; Laschi, F.; Zanello, P. Anodically-induced metal deprotonation of the hydrido complexes [{PCH$_2$CH$_2$PPh$_2$)$_3$}M(H)Cl] (M = Fe, Ru, Os): the first step to the electrogeneration of Fe(I),Ru(I) and Os(I) five-coordinate complexes. *Inorg. Chim. Acta* 1997, *259*, 61-70.

(11) Wagner, H. K.; Wadepohl, H.; Ballmann, J. A 2,2′-diphosphinotolane as a versatile precursor for the synthesis of P-ylidic mesoionic carbenes via reversible C–P bond formation. *Chem. Sci.* 2021, *12*, 3693-3701.

(12) (a) Eberle, L.; Kreis, F.; Stein, C. A. M.; Mörsdorf, J.-M.; Ballmann, J. [AsCCAs]-Coordinated Rhenium Hydrides and Their Reactivities Toward Unsaturated Hydrocarbons, Heterocumulenes, and CO$_2$. *Inorg. Chem.* 2023, *62*, 8635-8646; (b) Rudin, B.; Eberle, L.; Ballmann, J. 2,2′-Diphosphino- and 2,2′-Diarsenotolanes and Their Fe-, Co-, and Ni-Complexes: Pnictogen-Dependent Cyclization Tendencies and Metal-Dependent Stability and Reactivity Patterns. *Organometallics* 2023, *42*, 933-943; (c) Eberle, L.; Lindenthal, S.; Ballmann, J. To Split or Not to Split: [AsCCAs]-Coordinated Mo, W, and Re Complexes and Their Reactivity toward Molecular Dinitrogen. *Inorg. Chem.* 2024, *63*, 3682-3691.

(13) Dinuclear Ru(II) complexes with similar [Ru(μ-Cl)$_3$Ru]$^+$ cores are known; see for example: (a) Field, L. D.; Messerle, B. A.; Soler, L.; Buys, I. E.; Hambley, T. W. Polypyrazolylmethane complexes of ruthenium *J. Chem. Soc., Dalton Trans.* 2001, 1959-1965; (b) Rozenel, S. S.; Arnold, J. Bimetallic Ruthenium PNP Pincer Complex As a Platform to Model Proposed Intermediates in Dinitrogen Reduction to Ammonia. *Inorg. Chem.* 2012, *51*, 9730-9739; (c) Sgro, M. J.; Stephan, D. W. Synthesis and reactivity of ruthenium tridentate bis-phosphinite ligand complexes. *Dalton Trans.* 2013, *42*, 10460-10472; (e) Phanopoulos, A.; White, A. J. P.; Long, N. J.; Miller, P. W. Catalytic Transformation of Levulinic Acid to 2-Methyltetrahydrofuran Using Ruthenium–*N*-Triphos Complexes. *ACS Catalysis* 2015, *5*, 2500-2512; (d) Deng, L.; Kang, B.; Englert, U.; Klankermayer, J.; Palkovits, R. Direct Hydrogenation of Biobased Carboxylic Acids Mediated by a Nitrogen-centered Tridentate Phosphine Ligand. *ChemSusChem* 2016, *9*, 177-180; (e) Saha, R.; Mukherjee, A.; Bhattacharya, S. Di-ruthenium complexes of 1,4-diazabutadiene ligands: synthesis, characterization and utilization as catalyst precursors for the oxidative coupling of amines to imines in air. *New J. Chem.* 2023, *47*, 12709-12717.

(14) (a) Weigend, F.; Ahlrichs, R. Balanced basis sets of split valence, triple zeta valence and quadruple zeta valence quality for H to Rn: Design and assessment of accuracy. *Phys. Chem. Chem. Phys.* 2005, *7*, 3297-3305; (b) Weigend, F. Accurate Coulomb-fitting basis sets for H to Rn. *Phys. Chem. Chem. Phys.* 2006, *8*, 1057-1065; (c) Grimme, S.; Antony, J.; Ehrlich, S.; Krieg, H. A consistent and accurate ab initio parametrization of density functional dispersion correction (DFT-D) for the 94 elements H-Pu. *J. Chem. Phys.* 2010, *132*, 154104; (d) Grimme, S.; Ehrlich, S.; Goerigk, L. Effect of the damping function in dispersion corrected density functional theory. *J. Comput. Chem.* 2011, *32*, 1456-1465; (e) Neese, F.; Wennmohs, F.; Becker, U.; Riplinger, C. The ORCA quantum chemistry program package. *J. Chem. Phys.* 2020, *152*, 224108.

(15) Attempts to record cyclic voltammograms for compounds 3-E in MeCN were hampered as a number of new peaks appeared in each case (E = P, As) after the first cycle. It is assumed that this observation is related to a partial exchange of the chlorides in 3-E for [PF$_6$]$^-$ counterions, stemming from the electrolyte (NBu$_4$PF$_6$).

(16) It was also shown that 7-P is present in the mixtures obtained after oxidation of 3-P given that a very few single crystals of 7-P separated serendipitously from the crude reaction mixture. Although the molecular structure of 7-P was thus confirmed (see SI for details), pure batches of 7-P were not obtained.

(17) (a) Stoychev, G. L.; Auer, A. A.; Neese, F. Automatic Generation of Auxiliary Basis Sets. *J. Chem. Theory Comput.* 2017, *13*, 554-562; (b) Rolfes, J. D.; Neese, F.; Pantazis, D. A. All-electron scalar relativistic basis sets for the elements Rb–Xe. *J. Comput. Chem.* 2020, *41*, 1842-1849.

(18) Evans, D. F. The determination of the paramagnetic susceptibility of substances in solution by nuclear magnetic resonance. *J. Chem. Soc.* 1959, 2003-2005.

(19) Singh, S. K.; Eng, J.; Atanasov, M.; Neese, F. Covalency and chemical bonding in transition metal complexes: An ab initio based ligand field perspective. *Coord. Chem. Rev.* 2017, *344*, 2-25.

(20) Akhbari, K.; Morsali, A. Thallium(I) supramolecular compounds: Structural and properties consideration. *Coord. Chem. Rev.* 2010, *254*, 1977-2006.

(21) (a) Jeffery, J. C.; Jelliss, P. A.; Liao, Y.-H.; Stone, F. G. A. Carborane complexes of ruthenium: studies on the chemistry of the Ru(CO)$_2$(η^5-7,8-Me$_2$-7,8-C$_2$B$_9$H$_9$) fragment and the X-ray crystal structure of [NEt$_4$][Ru$_2$(μ-Tl)(CO)$_4$(η^5-7,8-Me$_2$-7,8-C$_2$B$_9$H$_9$)$_2$]. *J. Organomet. Chem.* 1998, *551*, 27-36; (b) Bytheway, I.; Griffith, C. S.; Koutsantonis, G. A.; Skelton, B. W.; White, A. H. A Linear Ru-Tl-Ru Complex Obtained from Halide Abstraction: An Example of Metal-Dative Bonding. *Eur. J. Inorg. Chem.* 2007, 3240-3246; (c) Bai, W.; Zhang, J.-X.; Fan, T.; Tse, S. K. S.; Shou, W.; Sung, H. H. Y.; Williams, I. D.; Lin, Z.; Jia, G. Syntheses and Structures of Ruthenium Complexes Containing a Ru-H-Tl Three-Center–Two-Electron Bond. *Angew. Chem. Int. Ed.* 2018, *57*, 12874-12879.

(22) (a) Bader, R. F. W. A quantum theory of molecular structure and its applications. *Chem. Rev.* 1991, *91*, 893-928; (b) Bader, R. F. W. The Quantum Mechanical Basis of Conceptual Chemistry. *Monatsh. Chem.* 2005, *136*, 819-854.

(23) Compound 10 may be interpreted as a Tl(I) cation captured between two neutral Ru(I) fragments, which – at a first glance – may suggest that both Ru(I) halves are antiferromagnetically coupled via the Tl(I)-bridge to eventually form the experimentally observed diamagnetic compound. Biased by this interpretation, we launched an extensive search for an open-shell singlet using a broken-symmetry BS(1,1) ansatz. These efforts, however, were unsuccessful as all our attempts using different functionals and starting geometries ultimately converged to closed-shell singlet solutions. These closed shell-solutions were analyzed via QTAIM, NBO and IBO, which led to our proposal that the Ru–Tl–Ru motif in 10 is best described as a 3*c*-4*e*$^-$ bond.

(24) (a) Bader, R. F. W. Bond Paths Are Not Chemical Bonds. *J. Phys. Chem. A* 2009, *113*, 10391-10396; (b) Grimme, S.; Mück-Lichtenfeld, C.; Erker, G.; Kehr, G.; Wang, H.; Beckers, H.; Willner, H. When Do Interacting Atoms Form a Chemical Bond? Spectroscopic Measurements and Theoretical Analyses of Dideuteriophenanthrene. *Angew. Chem. Int. Ed.* 2009, *48*, 2592-2595; (c) Shahbazian, S. Why Bond Critical Points Are Not "Bond" Critical Points. *Chem. – Eur. J.* 2018, *24*, 5401-5405.

(25) Molina Molina, J.; Dobado, J. A. The three-center-four-electron (3c-4e) bond nature revisited. An atoms-in-molecules theory (AIM) and ELF study. *Theor. Chem. Acc.* 2001, *105*, 328-337.

(26) (a) Poater, J.; Solà, M.; Duran, M.; Fradera, X. The calculation of electron localization and delocalization indices at the Hartree–Fock, density functional and post-Hartree–Fock levels of theory. *Theor. Chem. Acc.* 2002, *107*, 362-371;(b) Lu, T.; Chen, F. Multiwfn: A multifunctional wavefunction analyzer. *J. Comput. Chem.* 2012, *33*, 580-592.

(27) Reiersølmoen, A. C.; Battaglia, S.; Øien-Ødegaard, S.; Gupta, A. K.; Fiksdahl, A.; Lindh, R.; Erdélyi, M. Symmetry of three-center, four-electron bonds. *Chem. Sci.* 2020, *11*, 7979-7990.

(28) (a) Knizia, G. Intrinsic Atomic Orbitals: An Unbiased Bridge between Quantum Theory and Chemical Concepts. *J. Chem. Theory Comput.*

2013, *9*, 4834-4843; (b) Knizia, G.; Klein, J. E. M. N. Electron Flow in Reaction Mechanisms – Revealed from First Principles. *Angew. Chem. Int. Ed.* 2015, *54*, 5518-5522.